JCTC Journal of Chemical Theory and Computation

Energy-Represented Direct Inversion in the Iterative Subspace within a Hybrid Geometry Optimization Method

Xiaosong Li*

Department of Chemistry, University of Washington, Seattle, Washington 98195-1700

Michael J. Frisch

Gaussian, Inc., Wallingford, Connecticut 06492

Received November 8, 2005

Abstract: A geometry optimization method using an energy-represented direct inversion in the iterative subspace algorithm, GEDIIS, is introduced and compared with another DIIS formulation (controlled GDIIS) and the quasi-Newton rational function optimization (RFO) method. A hybrid technique that uses different methods at various stages of convergence is presented. A set of test molecules is optimized using the hybrid, GEDIIS, controlled GDIIS, and RFO methods. The hybrid method presented in this paper results in smooth, well-behaved optimization processes. The optimization speed is the fastest among the methods considered.

I. Introduction

Geometry optimization is an essential part of computational chemistry. Any theoretical investigation that involves calculations of transition structures, barrier heights, heats of reaction, or vibrational spectra requires searches for one or more minima or saddle points on a potential energy surface (PES). Computational methods are applied to large systems of ever-increasing size. Biomolecules, polymers, and nanostructures with hundreds to thousands of atoms are often difficult to optimize because of excessive degrees of freedom. Any decrease in the computational cost and increase in the general stability of geometry optimization would be welcome.

A variety of algorithms for geometry optimization are widely used in computational chemistry (for some recent reviews, see refs 1 and 2). Geometry optimization methods can be broadly classified into two major categories. First-order methods use only analytic first derivatives to search for stationary points; second-order methods use analytic first and second derivatives, assuming a quadratic model for the potential energy surface and a Newton−Raphson step for the minima search

$$\Delta x = -\mathbf{H}^{-1}\mathbf{g} \tag{1}$$

where $\mathbf{g}$ is the gradient (first derivative) and $\mathbf{H}^{-1}$ is the inverse Hessian (second derivative). While second-order optimization schemes need fewer steps to reach convergence than first-order methods,[3] this approach can quickly become very expensive with increasing system size because the explicit computation of the Hessian scales as $O(N^4)-O(N^5)$, where N is a measure of the system size. Quasi-Newton methods are intermediate between the first- and second-order approaches. An initial estimate of the Hessian is obtained by some inexpensive method. Subsequently, the Hessian is updated using the first derivatives and displacements, by methods such as BFGS,[4−7] SR1,[8] and PSB.[9,10] The quasi-Newton approach is comparable in computational cost to first-order methods and in convergence speed to second-order methods.

The use of a Newton−Raphson step when the PES is far away from a quadratic region can lead to overly large step sizes in the wrong direction. The stability of a Newton−Raphson geometry optimization can be enhanced by controlling the step size using techniques such as rational function optimization (RFO)[11,12] and the trust radius model.[1−3,13−16] To reduce the number of iterations required to reach convergence, a least-squares minimization scheme is used: direct inversion in the iterative subspace (DIIS).[17,18] The DIIS approach is efficient in both converging the wave function[17−21] and optimizing the geometry.[22,23] It extrapolates/interpolates a set of vectors $\{\mathbf{R}_i\}$ by minimizing the errors in the least-

* Corresponding author. Fax: 206-685-8665. E-mail: li@chem.washington.edu.

10.1021/ct050275a CCC: $33.50
Published on Web 04/18/2006

squares sense (for a leading reference, see ref 17):

$$\mathbf{A} = \begin{pmatrix} a_{1,1} & \cdots & a_{1,N} & 1 \\ \vdots & \ddots & \vdots & \vdots \\ a_{N,1} & \cdots & a_{N,N} & 1 \\ 1 & \cdots & 1 & 0 \end{pmatrix}$$

$$\begin{pmatrix} a_{1,1} & \cdots & a_{1,N} & 1 \\ \vdots & \ddots & \vdots & \vdots \\ a_{N,1} & \cdots & a_{N,N} & 1 \\ 1 & \cdots & 1 & 0 \end{pmatrix} \begin{pmatrix} c_1 \\ \vdots \\ c_N \\ \lambda \end{pmatrix} = \begin{pmatrix} 0 \\ \vdots \\ 0 \\ 1 \end{pmatrix} \text{ and } \sum c_i = 1 \qquad (2)$$

where λ is the Lagrangian multiplier. The coefficients minimize a working function, which can be an error function[17,18,21−23] or an energy function.[19,20] Fock matrix and nuclear positions are often chosen as the vectors for self-consistent field (SCF)[17,18,20,21] and geometry[22,23] optimizations, respectively. When the working function is an error function, the matrix **A** is usually defined as the product of error vectors, $a_{i,j} = e_i e_j^{\mathrm{T}}$, where the error vector can be a quasi-Newton step for geometry optimization[22,23] or the commutator [**F**, **P**] for SCF convergence.[17,18] Solving eq 2 leads to a set of DIIS coefficients c_i that are used to obtain a new vector, $\mathbf{R^*} = \sum_i c_i \mathbf{R}_i$, which has the minimum functional value within the search space. Direct solution of eq 2 often leads to unproductive oscillations when optimizing large systems.[20,23] Farkas and Schlegel have introduced some controls to ensure a downhill DIIS extrapolation/interpolation for geometry optimization (GDIIS).[23] Scuseria and co-workers have introduced a stable and efficient alternative DIIS formalism for SCF convergence, energy-DIIS (SCF-EDIIS).[19,20] The SCF-EDIIS algorithm minimizes an energy function and enforces coefficients to be positive definite.

This paper extends the energy-represented direct inversion in the iterative subspace algorithm from SCF convergence to geometry optimization (GEDIIS). A hybrid geometry optimization technique that utilizes the advantages of different methods of various stages of the optimization is then illustrated and tested.

II. Methodology and Benchmarks

Optimizations are carried out using the development version of the Gaussian series of programs[24] with the addition of the geometry optimization algorithms using GEDIIS and the hybrid method presented here. For all methods, the geometry optimization is considered converged when the root-mean-square (RMS) force is less than 1×10^{-5} au, the RMS geometry displacement is less than 4×10^{-5} au, the maximum component of the force vector is less than 1.5×10^{-5} au, and the maximum component of the geometry displacement is less than 6×10^{-5} au. All calculations are carried out with redundant internal coordinates. No symmetry operations or reorientations are imposed. Starting geometries are available upon request (li@chem.washington.edu).

A. Geometry Optimization Using Energy-Represented Direct Inversion in the Iterative Subspace (GEDIIS). As in all DIIS-based schemes, the GEDIIS formalism yields a new vector **R*** constructed from a linear combination of N previously computed vectors $\mathbf{R}_i$

$$\mathbf{R^*} = \sum_{i=1}^{N} c_i \mathbf{R}_i, \qquad \sum_{i=1}^{N} c_i = 1 \qquad (3)$$

In GEDIIS, $\mathbf{R}_i$'s are geometries and c_i's minimize an energy function. The energy of the new structure **R*** can be approximated to first order with an expansion at $\mathbf{R}_i$

$$E(\mathbf{R^*}) = E(\mathbf{R}_i) + (\mathbf{R^*} - \mathbf{R}_i)\mathbf{g}_i \qquad (4)$$

where $E(\mathbf{R}_i)$ and $\mathbf{g}_i$ are the energy and gradient of structure $\mathbf{R}_i$, respectively. Multiplying both sides of eq 4 by c_i, and summing over N points, we obtain

$$E(\mathbf{R^*}) = \sum_{i=1}^{N} c_i [E(\mathbf{R}_i) + \sum_{j=1}^{N} c_j \mathbf{R}_j \mathbf{g}_i - \mathbf{R}_i \mathbf{g}_i] \qquad (5)$$

A simple algebraic manipulation leads to the GEDIIS working function

$$E(\mathbf{R^*}) = \sum_{i=1}^{N} c_i E(\mathbf{R}_i) - \frac{1}{2}\sum_{i,j=1}^{N} c_i c_j [\mathbf{R}_i(\mathbf{g}_i - \mathbf{g}_j) + \mathbf{g}_i(\mathbf{R}_i - \mathbf{R}_j)] \qquad (6)$$

or

$$E(\mathbf{R^*}) = \sum_{i=1}^{N} c_i E(\mathbf{R}_i) - \frac{1}{2}\sum_{i,j=1}^{N} c_i c_j (\mathbf{g}_i - \mathbf{g}_j)(\mathbf{R}_i - \mathbf{R}_j)$$

where

$$\sum_{i=1}^{N} c_i = 1$$

The quadratic term in eq 6 represents the variations in energy for changes of geometric coordinates and gradients within the search space. Equation 6 is formally identical to Scuseria's SCF-EDIIS equation for wave-function optimization.[20] In both the GEDIIS and SCF-EDIIS formalisms, the energy function is minimized directly with respect to the expansion coefficients, c_i's. The working functions in GEDIIS, SCF-DIIS,[17,18] SCF-EDIIS,[20] and GDIIS[22,23] are all quadratic with respect to c_i, and minimizations are therefore performed in a least-squares sense. The comparison of this technique with Pulay's DIIS[17,18] has been discussed extensively in the literature.[19,20]

The set of DIIS coefficients, c_i's, that minimize the energy function, eq 6, are used to construct a new geometry **R*** from a linear combination of known points (eq 3). The resulting geometry **R*** is, to a first-order approximation, associated with the optimal energy within the search space. However, **R*** is not necessarily the final minimum structure. The distance from **R*** to the minimum structure can be approximated by a second-order Newton step. In this work, we use a RFO step for the second-order correction

$$\mathbf{R}_{N+1} = \mathbf{R^*} + \Delta\mathbf{R} = \sum_{i=1}^{N} c_i \mathbf{R}_i - \sum_{i=1}^{N} c_i \mathbf{g}_i (\mathbf{H} - \xi)^{-1} \qquad (7)$$

where the parameter ξ is optimized using the RFO approach

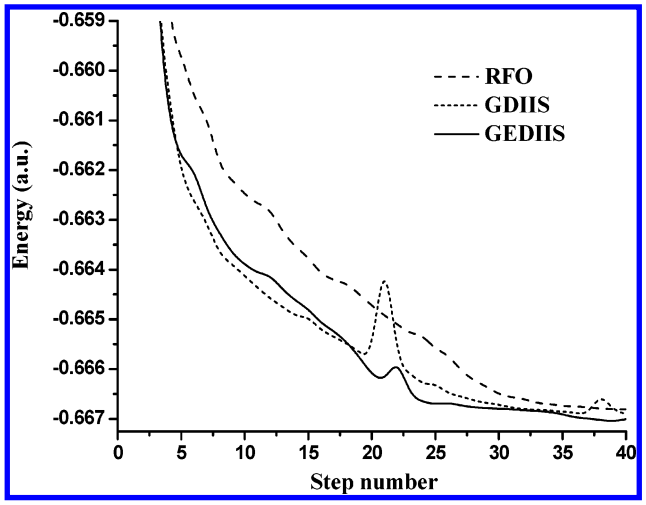

Figure 1. Energy vs step number for geometry optimizations on taxol at AM1.

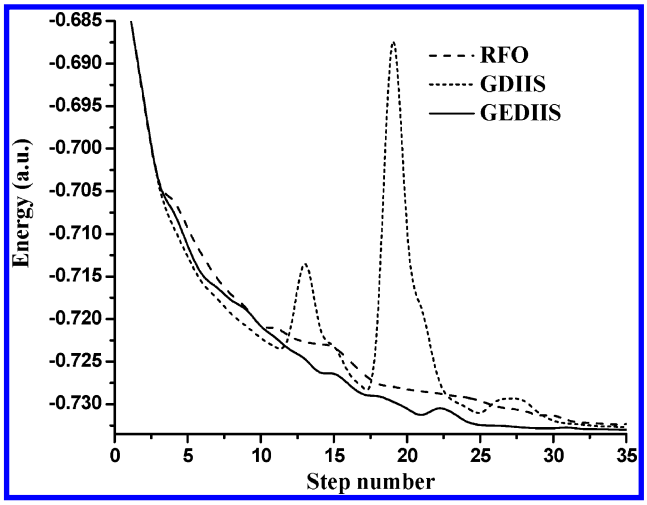

Figure 2. Energy vs step number for geometry optimizations on For−$(Ala)_{10}$−NH_2 at AM1.

(note that the Hessian is a constant in a quadratic approximation).[11,12] With no constraint on the sign of c_i, eq 7 is essentially an extrapolation; when $c_i > 0$, it becomes an interpolation step. When the molecular geometry is far from convergence, extrapolations can lead to erroneously large steps away from the optimized geometry. To ensure optimization stability, an enforced interpolation constraint, $c_i > 0$, is added into eq 2 (for detailed machinery, see ref 20). As a result, GEDIIS searches for a new geometry in the region close to the local potential energy surface, that is, interpolations only.

We update the geometric Hessian with first derivatives: a weighted combination of BFGS and SR1[23] with the square root of the Bofill[25] weighting factor

$$\mathbf{H}_i = \mathbf{H}_{i-1} + \varphi\Delta\mathbf{H}_i^{\mathrm{SR1}} + (1-\varphi)\Delta\mathbf{H}_i^{\mathrm{BFGS}}$$

$$\Delta\mathbf{H}_i^{\mathrm{SR1}} = -\frac{(\mathbf{H}_{i-1}\Delta\mathbf{R}_{i-1} - \Delta\mathbf{g}_i)(\mathbf{H}_{i-1}\Delta\mathbf{R}_{i-1} - \Delta\mathbf{g}_i)^{\mathrm{T}}}{(\mathbf{H}_{i-1}\Delta\mathbf{R}_{i-1} - \Delta\mathbf{g}_i)^{\mathrm{T}}\Delta\mathbf{R}_{i-1}}$$

$$\Delta\mathbf{H}_i^{\mathrm{BFGS}} = \frac{\Delta\mathbf{g}_i\Delta\mathbf{g}_i^{\mathrm{T}}}{\Delta\mathbf{R}_{i-1}^{\mathrm{T}}\Delta\mathbf{g}_i} - \frac{\mathbf{H}_{i-1}\Delta\mathbf{R}_{i-1}\Delta\mathbf{R}_{i-1}^{\mathrm{T}}\mathbf{H}_{i-1}}{\Delta\mathbf{R}_{i-1}^{\mathrm{T}}\mathbf{H}_{i-1}\Delta\mathbf{R}_{i-1}}$$

$$\varphi = \sqrt{\varphi^{\mathrm{Bofill}}} = \sqrt{\frac{[(\mathbf{H}_{i-1}\Delta\mathbf{R}_{i-1} - \Delta\mathbf{g}_i)^{\mathrm{T}}\Delta\mathbf{R}_{i-1}]^2}{(\mathbf{H}_{i-1}\Delta\mathbf{R}_{i-1} - \Delta\mathbf{g}_i)^{\mathrm{T}}(\mathbf{H}_{i-1}\Delta\mathbf{R}_{i-1} - \Delta\mathbf{g}_i)\Delta\mathbf{R}_{i-1}^{\mathrm{T}}\Delta\mathbf{R}_{i-1}}}$$

$$\Delta\mathbf{g}_i = \mathbf{g}_i - \mathbf{g}_{i-1}$$

$$\Delta\mathbf{R}_i = \mathbf{R}_i - \mathbf{R}_{i-1} \qquad (8)$$

Equation 8 has been successfully used for large-molecule geometry optimization.[26]

Figures 1 and 2 show energy profiles for the first 40 optimization steps of taxol and For−$(Ala)_{10}$−NH_2 using RFO, GDIIS, and GEDIIS methods at the AM1 level of theory. The GEDIIS method reduces, or even eliminates, large energy oscillations, which often appear in GDIIS at the early stage of optimization because of large extrapolation steps. The convergence behavior of the GEDIIS approach is generally smooth and well-behaved. Note that GEDIIS shows small bumps at places similar to those in GDIIS, indicating that it is taking approximately the same path but in a more controlled fashion. This enhanced stability is a result of the better representation of error vectors and the enforced DIIS interpolation. The SCF-EDIIS method for wave-function optimization also shows enhanced stability.[20] Because the DIIS algorithm collects information from previously computed points for a better picture of the local potential surface than that obtained from a single point, as in the RFO method, the potential energies at the same optimization step are generally in the order $E_{\mathrm{GEDIIS}} < E_{\mathrm{GDIIS}} < E_{\mathrm{RFO}}$.

B. Mixed Geometry Optimization Scheme. The simple RFO, GDIIS, and GEDIIS methods each perform best in different stages of the geometry optimization. Even though GEDIIS exhibits fast and smooth behavior at the early stage of geometry optimization, the first-order energy-represented **A** matrix has no knowledge of the curvature of the local potential surface, so the problems of gradient-based methods are still present in a direct implementation of the GEDIIS method presented here. In a well-behaved quadratic region near convergence, first-derivative-based optimizations such as GEDIIS are generally slower than those using both first and second derivatives. To take advantage of the fast convergence of Hessian-based methods near minima, GDIIS using RFO steps as error vectors can be used instead of GEDIIS when the optimization process is close to convergence. Another critical problem for methods using DIIS minimization schemes results from interpolation where the optimization scope is limited to neighboring potential surfaces only: optimizations can easily be trapped in undesired shallow potential wells. This is particularly troublesome for optimizing large molecules with many degrees of freedom. By contrast, RFO is essentially a single extrapolation step that is better able to overcome shallow potential wells. Therefore, it is a reasonable strategy to use RFO as a *preoptimizer* or *potential well selector* followed by DIIS-based optimization methods.

We thus combine methods to gain a fast hybrid geometry optimization scheme: (1) The geometry optimization begins with the RFO method to use the Hessian-based quadrature

Table 1. Comparison of the Computational Costs for Quasi-Newton RFO, Controlled GDIIS, GEDIIS, and Hybrid Optimization Methods on Select Baker Test Molecules

		RFO		GDIIS		GEDIIS		hybrid	
	E^a (au)	T^b	N^c	T^b	N^c	T^b	N^c	T^b	N^c
disilyl ether	−657.881 31	1.28	13	1.18	12	1.10	11	1.00	10
1,3,5-trisilaceyclohexane	−990.064 87	1.10	12	0.93	10	1.07	12	1.00	11
2-hydroxybicyclopentane	−270.492 14	1.14	15	0.99	13	1.00	13	1.00	13
achtar10	−363.046 87	1.27	18	1.06	15	1.00	14	1.00	14
benzidine	−574.008 39	1.08	12	1.00	11	1.01	11	1.00	11
pterin	−580.647 03	1.00	12	1.01	12	1.01	12	1.00	12
histidine	−548.755 26	1.01	17	1.00	17	1.00	17	1.00	17
caffeine	−680.376 96	1.00	11	1.00	11	0.86	9	1.00	11
menthone	−467.143 10	1.00	14	1.00	14	0.95	13	1.00	14
acthcp	−852.314 18	1.05	17	1.00	16	1.00	16	1.00	16
histamine H^+	−360.593 73	1.06	16	0.92	14	0.92	14	1.00	15
hydrazobenzene	−573.970 61	1.00	20	1.10	22	1.41	28	1.00	20

[a] Final energy. [b] Total CPU time with respect to that of the hybrid method. [c] Number of optimization steps.

Table 2. Comparison of the Computational Costs for Quasi-Newton RFO, Controlled GDIIS, GEDIIS, and Hybrid Optimization Methods

	histidine (20 atoms)	hydrazobenzene (26 atoms)	taxol (113 atoms)	For−$(Ala)_{10}$−NH_2 (106 atoms)	For−$(Ala)_{20}$−NH_2 (206 atoms)
	MP2/6-311G(d)	B3LYP/6-31G(d)	PBEPW91/3-21G	HF/STO-3G	AM1
			Final Energy		
RFO	−545.663 46	−573.970 61	−2911.140 32	−2593.884 16	−1.425 66
GDIIS	−545.663 46	−573.970 61	−2911.140 33	−2593.882 62	−1.425 66
GEDIIS	−545.663 46	−573.970 61	−2911.140 33	−2593.882 58	−1.425 66
hybrid	−545.663 46	−573.970 61	−2911.140 33	−2593.884 16	−1.425 66
			Number of Optimization Steps		
RFO	21	20	135	94	107
GDIIS	21	22	136	111	92
GEDIIS	16	28	125	67	88
hybrid	19	20	105	79	91
			Relative CPU Times[a]		
RFO	1.10	1.00	1.22	1.11	1.13
GDIIS	1.10	1.10	1.30	1.47[b]	1.02
GEDIIS	0.85	1.41	1.19	0.81[b]	0.96
hybrid	1.00	1.00	1.00	1.00	1.00

[a] Total CPU time with respect to that of the hybrid method. [b] Minima higher in energy than that optimized by the hybrid method.

to avoid shallow potential wells; (2) the optimization algorithm switches to fast and smoothly converging GEDIIS when the root-mean-square force of the latest point is smaller than 10^{-2} au; (3) when the root-mean-square RFO step of the latest point is less than 2.5×10^{-3} au, GDIIS[23] is used until convergence. This hybrid method takes advantage of the three methods considered here—the ability to overcome shallow potential wells by RFO, smooth optimization by GEDIIS, and fast convergence of RFO−DIIS near the minimum. The switching criteria were optimized from tests on the Baker set (Table 1).[27] Figure 3 illustrates optimizations using RFO, GDIIS, GEDIIS, and the hybrid method for For−$(Ala)_{10}$−NH_2 at the HF/STO-3G level of theory. Both GDIIS and GEDIIS converge to a minimum that is about 1.5×10^{-3} au higher in energy than that by RFO. The smallest harmonic frequency for the DIIS minimum is only about 7 cm^{-1}, indicating a very flat potential well. The hybrid optimization switches to GEDIIS from RFO after the first 20 steps and switches to GDIIS after another 26 steps. Convergence is reached within 79 steps, significantly faster than the 94 steps by RFO. While the DIIS methods remain at a higher energy minimum, the hybrid method overcomes

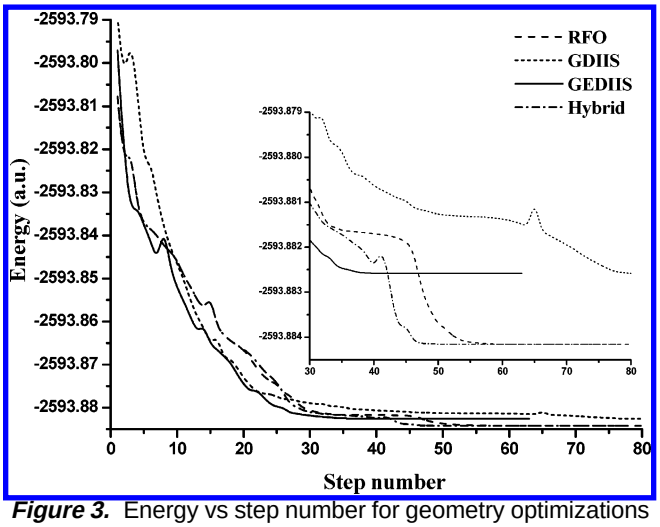

Figure 3. Energy vs step number for geometry optimizations on For−$(Ala)_{10}$−NH_2 at HF/STO-3G.

the shallow potential well and optimizes For−$(Ala)_{10}$−NH_2 to the RFO minimum.

Table 2 compares final energies and computational costs by the RFO, GDIIS, GEDIIS, and hybrid optimization methods on select molecules at various levels of theory. The computational costs are presented as the relative CPU times. The hybrid method introduced in this paper is the fastest among the popular geometry optimization methods considered here. Most importantly, the optimization behavior of the hybrid method is consistently smooth and fast through optimizations of the Baker set and large biochemical molecules tested in this paper.

III. Conclusion

This paper presents a geometry optimization method using GEDIIS. The GEDIIS method minimizes an energy representation of the local potential energy surface in the vicinity of previously computed points (gradients and geometries) as a least-squares problem. The enforced interpolation in GEDIIS leads to enhanced stability.

A hybrid geometry optimization algorithm is proposed that takes into account the problems and advantages of different optimization methods. The hybrid method starts off with RFO as a *preoptimizer* and switches to GEDIIS when a certain convergence threshold is met. Near the minimum, GEDIIS switches to RFO−DIIS. This takes advantage of RFO's ability to overcome shallow potential wells, smooth optimization by GEDIIS, and fast convergence of RFO−DIIS near the minimum. Optimizations of test molecules with the hybrid method are shown to be smooth, reliable, and fast.

Acknowledgment. The authors are grateful for discussions with Professor Schlegel at Wayne State University.

References

(1) Schlegel, H. B. Geometry Optimization on Potential Energy Surfaces. In *Modern Electronic Structure Theory*; Yarkony, D. R., Ed.; World Scientific: Singapore, 1995; p 459.

(2) Schlegel, H. B. Geometry Optimization. In *Encyclopedia of Computational Chemistry*; Schleyer, P. v. R., Allinger, N. L., Kollman, P. A., Clark, T., Schaefer, H. F., III, Gasteiger, J., Schreiner, P. R., Eds.; Wiley: Chichester, U. K., 1998; Vol. 2, p 1136.

(3) Fletcher, R. *Practical Methods of Optimization*; Wiley: Chichester, U. K., 1981.

(4) Broyden, C. G. *J. Inst. Math. Appl.* **1970**, *6*, 76.

(5) Fletcher, R. *Comput. J. (Switzerland)* **1970**, *13*, 317.

(6) Goldfarb, D. *Math. Comput.* **1970**, *24*, 23.

(7) Shanno, D. F. *Math. Comput.* **1970**, *24*, 647.

(8) Murtagh, B.; Sargent, R. W. H. *Comput. J. (Switzerland)* **1972**, *13*, 185.

(9) Powell, M. J. D. *Nonlinear Programing*; Academic: New York, 1970.

(10) Powell, M. J. D. *Math. Program.* **1971**, *1*, 26.

(11) Banerjee, A.; Adams, N.; Simons, J.; Shepard, R. *J. Phys. Chem.* **1985**, *89*, 52.

(12) Simons, J.; Nichols, J. *Int. J. Quantum Chem.* **1990**, *24*, 263.

(13) Murray, W.; Wright, M. H. *Practical Optimization*; Academic: New York, 1981.

(14) *Nonlinear Optimization*; Powell, M. J. D., Ed.; Academic: New York, 1982.

(15) Dennis, J. E.; Schnabel, R. B. *Numerical Methods for Unconstrained Optimization and Nonlinear Equations*; Prentice Hall: Upper Saddle River, New Jersey, 1983.

(16) Scales, L. E. *Introduction to Nonlinear Optimization*; Macmillam: Basingstoke, England, 1985.

(17) Pulay, P. *Chem. Phys. Lett.* **1980**, *73*, 393.

(18) Pulay, P. *J. Comput. Chem.* **1982**, *3*, 556.

(19) Cancès, E.; Le Bris, C. *Int. J. Quantum Chem.* **2000**, *79*, 82.

(20) Kudin, K. N.; Scuseria, G. E.; Cancès, E. *J. Chem. Phys.* **2002**, *116*, 8255.

(21) Li, X.; Millam, J. M.; Scuseria, G. E.; Frisch, M. J.; Schlegel, H. B. *J. Chem. Phys.* **2003**, *119*, 7651.

(22) Csaszar, P.; Pulay, P. *J. Mol. Struct.* **1984**, *114*, 31.

(23) Farkas, Ö.; Schlegel, H. B. *Phys. Chem. Chem. Phys.* **2002**, *4*, 11.

(24) Frisch, M. J.; Trucks, G. W.; Schlegel, H. B.; Scuseria, G. E.; Robb, M. A.; Cheeseman, J. R.; Montgomery, J. A., Jr.; Vreven, T.; Kudin, K. N.; Burant, J. C.; Millam, J. M.; Iyengar, S. S.; Tomasi, J.; Barone, V.; Mennucci, B.; Cossi, M.; Scalmani, G.; Rega, N.; Petersson, G. A.; Ehara, M.; Toyota, K.; Hada, M.; Fukuda, R.; Hasegawa, J.; Ishida, M.; Nakajima, T.; Kitao, O.; Nakai, H.; Honda, Y.; Nakatsuji, H.; Li, X.; Knox, J. E.; Hratchian, H. P.; Cross, J. B.; Adamo, C.; Jaramillo, J.; Cammi, R.; Pomelli, C.; Gomperts, R.; Stratmann, R. E.; Ochterski, J.; Ayala, P. Y.; Morokuma, K.; Salvador, P.; Dannenberg, J. J.; Zakrzewski, V. G.; Dapprich, S.; Daniels, A. D.; Strain, M. C.; Farkas, O.; Malick, D. K.; Rabuck, A. D.; Raghavachari, K.; Foresman, J. B.; Ortiz, J. V.; Cui, Q.; Baboul, A. G.; Clifford, S.; Cioslowski, J.; Stefanov, B. B.; Liu, G.; Liashenko, A.; Piskorz, P.; Komaromi, I.; Martin, R. L.; Fox, D. J.; Keith, T.; Al-Laham, M. A.; Peng, C. Y.; Nanayakkara, A.; Challacombe, M.; Gill, P. M. W.; Johnson, B.; Chen, W.; Wong, M. W.; Gonzalez, C.; Pople, *J. A. Development Version Rev. D01 ed.*; Gaussian, Inc.: Pittsburgh, PA, 2005.

(25) Bofill, J. M. *J. Comput. Chem.* **1994**, *15*, 1.

(26) Farkas, Ö.; Schlegel, H. B. *J. Chem. Phys.* **1999**, *111*, 10806.

(27) Baker, J. *J. Comput. Chem.* **1993**, *14*, 1085.

CT050275A